Formation of self-assembled polymeric complexes with bridged azido-dicarboxylato ligands

Assistant Lecturer Riyadh M. Ahmed
Professor Ahmed T. Numan
Professor Taki A. Himdan
Professor Mohamad J. Al-Jeboori
Department of Chemistry, College of Education, Ibn Al-Haitham
University of Baghdad

Abstract:

In this publication, several six coordinate bridged-polymeric metal complexes are reported. The reaction of 4,4`-dipyridine with ethyl chloroacetate in mole ratio of 1:2 gave the multidentate carboxylate ligand bis(N-carboxylatomethyl)-4,4`-dipyridinium). The reaction of the ligand with metal chloride and sodium azide resulted in the formation of the required polymeric complexes. Upon complex formation, the carboxylato ligand behaves as a neutral multidantate species. The mode of bonding and overall geometry of the complexes were determined through physico-chemical and spectroscopic methods. These studies revealed octahedral geometry about metal centres and complexes of the general formula $[Cr_2(L)(N_3)_4]Cl_2.H_2O$, $Na_2[Ag_2(L)(N_3)_4].H_2O$ and $[M_2(L)(N_3)_4].H_2O$ (where M = Mn, Fe, Co, Ni, Cu, Zn and Cd) were reported. These compounds were characterised by ^1H, ^{13}C NMR, mass spectroscopy, C.H.N, A.A., chloride content, magnetic susceptibility, melting point and molar conductance. Molecular structure for the complexes has been optimised by CS Chem 3D Ultra Molecular Modelling and Analysis Program and supported the formation of six coordinate polymeric complexes.

Keywords:

Polymeric complexes; Bridged azido-carboxylato ligands; Bis(N-carboxylatomethyl)4,4`-dipyridinium); Structural study.

Introduction:

The development of self-assembled polymeric species based on transition metal compounds and polydentate ligands are of current interest, due to their potential applications in supramolecular and environmental chemistry and medicine [1, 2]. One approach in supramolecular chemistry has been to develop coordination polymers with unique properties. The nature of the metal and the coordination fashion of the ligands has been facilitated to develop different synthetic strategies in design and synthesis of supramolecular structures with potential applications in photochemistry, molecular magnetism [3], catalysis [4], optoelectronic devices and clean energy including gas sorption and carbon capture [5]. The development in the design and synthesis of molecular magnetic materials has become an interested field in fabricating a number of new magnets. In particular, the developments of low-dimensional magnetic features one-dimensional (1D), or two-dimensional (2D), such as metamagnetism, bridge the gap between paramagnetism and three-dimensional (3D) long-range magnetic ordering [6-8]. Coordination chemistry provides an effective approach to design and prepare these low-dimensional magnetic systems when magnetic transition metal ions are assembled into coordination polymers by employing suitable ligands. The key to design such materials is to select short bridging ligands that can effectively mediate the magnetic coupling and construct novel structures [9]. The most used short bridging ligands include the cyanide, dicyanamide, carboxylate and azide. The carboxylate ligands are interested versatile species that used in the development of several directions in coordination chemistry. These approaches cover the preparation of building blocks of metal organic framework (MOFs) and to study the phenomenon of the antiferromagnetic interaction. The characteristic porous properties of the MOFs compounds allowed them to be used in the applications of hydrogen storage systems and carbon capture. On other hand, azide species is widely used in the coordination chemistry. The azide moiety can link metal ions in different fashion including a bridging mode. Depending on the coordination mode, complexes with particular structures and magnetic properties of the azido species are reported [10,11]. It is well documented that the magnetic exchange mediated *via* an azido bridge can be ferro- or antiferromagnetic, depending on the bridging mode and bonding parameters. The structures and thus the magnetic properties of metal azido systems are sensitive to the coligands employed in the system. Because of these facts, the design of self-assembled polymeric species containing mixed azido and carboxylato bridges are an interested area of research [12, 13]. In this work, we have explored the synthesis of dicarboxylate ligand and the role of metal ion in self-assembly process upon complex formation (Scheme 1). We also have investigated the influence of using the combination of azido and zwitterionic dicarboxylato bridges ligand on the structure and magnetic properties of polymeric self-assembled species.

Experimental

Materials and methods:

All reagents were obtained commercially (Aldrich) and used without further purification. Solvents used in the synthesis were distilled from appropriate drying agent immediately prior to use.

Physical measurements:

Elemental analyses (C, H and N) were carried out on a Heraeus instrument (Vario EL) at the University of the Manchester Metropolitan MMU) and Imperial College London (IC), UK. IR spectra were recorded as KBr discs using a Shimadzu 8400 S FTIR spectrophotometer from 4000-400 cm^{-1}. Melting points were obtained on an Electro-thermal Stuart melting point SMP40 capillary melting point apparatus and are uncorrected. Electronic spectra were measured from 200-1100 nm for 10^{-3} M solutions in DMSO at 25 °C using a Shimadzu 1800 spectrophotometer. ^{1}H- ^{13}C-NMR spectra were acquired in DMSO–d_6 solution using a Jeol 400 MHz spectrometer with tetramethylsilane (TMS) as an internal standard for ^{1}H NMR analysis at the MMU and IC, UK. Mass spectra for ligand and some metal complexes were obtained by positive Electron-Impact (EI), accurate Electrospray (ES) and Matrix Assisted Laser Desorption Ionisation Time of Flight MS (MALDI-TOF MS) was recorded on a VG autospec micromass spectrometer on BRUKER DALTONICS at the EPSRC Swansea, UK. The spectra were recorded at the EPSRC Swansea Mass Spectroscopy Facility, U.K. Metals were determined using a Shimadzu (A.A) 680 G atomic absorption spectrophotometer. Chloride was determined using potentiometer titration method on a 686-Titrp processor-665Dosimat-Metrohm Swiss. Conductivity measurements were made with DMSO solutions using a PW 9526 digital conductivity meter and room temperature magnetic moments were measured with a magnetic susceptibility balance (Johnson Matthey Catalytic System Division).

Synthesis

Preparation of the ligand:

The preparation of the ligand was adopted according to a published method [14] and as follows:

A solution of ethyl chloroacetate (2.46 g, 22 mmol) was added slowly to a mixture of 4,4`-bipyridine (2 g, 12 mmol) dissolved in acetone

(25 mL). The resulting solution was allowed to reflux for a three days. After the acetone was removed under reduced pressure a green residue was left, and then a mixture of HCl (50 mL, 5% w/v) was added. The resulting mixture was heated under reflux for 24 h to give a yellow solution. Removal of solvent afforded a yellow powdery product; yield (2.13 g, 66%). The product was then dissolved in (50 mL) of water, and silver(I) oxide (1.5 g, 0.0065 mmol) was added, with stirring, to remove the chloride ions. The white precipitate was filtered off, and the filtrate was then dried to yield a brownish solid, which was recrystallised from water/ethanol (1:4, v/v) to give ligand as a brownish solid; yield (1.61 g, 46%), m.p. = 246 °C. ^{1}H NMR data δ_H(400 MHz, DMSO-d_6, ppm), Figure (1), shows two conformation isomers A and B. Isomer A; 5.72 (4H, s, $C_{2, 2`}$-*H*), This peak is shifted downfield, in comparison with that in the free acetic acid, due to its attachment to the nitrogen atom, electron withdrawing group, and therefore the ($CH_2$) group is deshielded and appeared at a higher chemical shift, 8.71-8.73 (4H, d, J=6.87, $C_{4,4`,6,6`}$), 9.23-9.25 (4H, d, *J* =7.33, $C_{3, 3`,7, 7`}$). Isomer B; 5.78 (4H, s, $C_{2,2`}$), 8.63-8.65, and 8.85-8.87 (4H, d, J=7.33, $C_{4, 4`, 6, 6`}$), 8.78-8.79 (3H, d, J=6.87) and 9.18-9.20 (1H, d, J=6.87, $C_{3, 3`,7, 7`}$). The appearance of two isomers is perhaps due to the ease of rotation of the chelating portion of the molecule and/or the ease of rotation of the two pyridyl molecules; slow rotation could give one or two conformations that are not symmetrical. ^{13}C NMR data δ_c(400 MHz, DMSO-d_6, ppm), Figure (2), shows two chemical shift sets. Isomer A shows chemical shift at 60.01 ($C_{2, 2`}$), 126.59 ($C_{4, 4`, 6, 6`}$), 144.01 ($C_{3, 3`,7, 7`}$ ), 152.76 ($C_{5, 5`}$), 169.09 ($C_{1, 1`}$ ). Isomer B shows chemical shift at 60.92($C_{2, 2`}$), 126.80 ($C_{4, 4`, 6, 6`}$), 149.02 ($C_{3,3`,7,7`}$), 152.73 ($C_{5, 5`}$), 174.35 ($C_{1, 1`}$). The positive ES mass spectrum of the ligand Figure (3) and accurate mass Figure (4) showed the parent ion peak at 273 (24%) corresponding to M^+ ($C_{14}H_{12}N_2O_4$) and the following fragments at 243 (42 %) $[M-(CH_2O)]^+$; 215 (100) $[M-(CH_2O+CO)]^+$; 185 (5%) $[M-(CH_2O+CO+CH_2O)]^+$; 157 (50%) $[M-(CH_2O+ CO+ CH_2O+ CH_2O)]^+$.

General synthesis of polymeric complexes with ligand (L):

A mixture of metal chloride (1 mmol), L (1 mmol) and NaN_3 (2 mmol) in water/ethanol (50 mL, 4:6 v/v) was stirred for 30 min at room temperature, and then the mixture was refluxed for 30 min. Slow evaporation of the solution at room temperature yielded coloured crystals of the required complex within two weeks. Crystals were washed with methanol (2 mL) and 5 mL of diethylether, and then dried under vaccu. Elemental analysis data, colours, and yields for the complexes are given in (Table 1).

Molecular modelling:

3D molecular modelling of the proposed structure of the complexes was performed using CS Chem 3D Ultra Molecular Modelling and Analysis Program [15]. This programme is an interactive graphics analysis that allows rapid structure building, geometry optimization with minimum energy and molecular display. It is well known program and has the ability to handle polymeric transition metal complexes [16]. The correct stereochemistry was assured through the manipulation and modification of the molecular coordinates to obtain reasonable low energy molecular geometries.

Results and discussion

Chemistry:

The reaction of 4,4`-dipyridine with ethyl chloroacetate in mole ratios of 1:2 gave the multidentate carboxylate ligand bis(N-carboxylatomethyl)-4,4`-dipyridinium) L, in moderate yield (Scheme 1). The ligand was characterised by elemental analysis (Table 1), IR (Table 2), UV–Vis (Table 3) spectroscopy, ^1H, ^{13}C NMR and mass spectrometry. The NMR and the EI (+) mass spectra of the ligand were consistent with the proposed structural formula (see experimental section). The neutral and di-electrolyte polymeric complexes were synthesised by mixing at RT a 1 mmole of the appropriate ligand with 1 mmole of the metal chloride in a mixture of water: ethanol (4:6) followed by a solution of the sodium azide (2 mmol) in water. Complexes of the general formulae $[Cr_2(L)(N_3)_4]Cl_2.H_2O$, $Na_2[Ag_2(L)(N_3)_4].H_2O$ and $[M_2(L)(N_3)_4].H_2O$ (where M = Mn(II), Fe(II), Co(II), Ni(II), Cu(II), Zn(II) and Cd(II)) were obtained (Scheme 1). The complexes are air-stable solids, soluble with heat in DMSO, partially soluble in DMF and not soluble in other common organic solvents. The coordination geometries of the complexes were deduced from their spectra. The analytical data (Table 1) agree well with the suggested formulae. Conductivity measurements of the Cr(III) and Ag (I) bridged-complexes lie in the 72.11 and 76.09 $cm^2\Omega^{-1}mol^{-1}$ range, respectively indicating their 1:2 electrolytic behaviour. Non-electrolyte conductance behaviour for other complexes was observed (Table 1) [17].

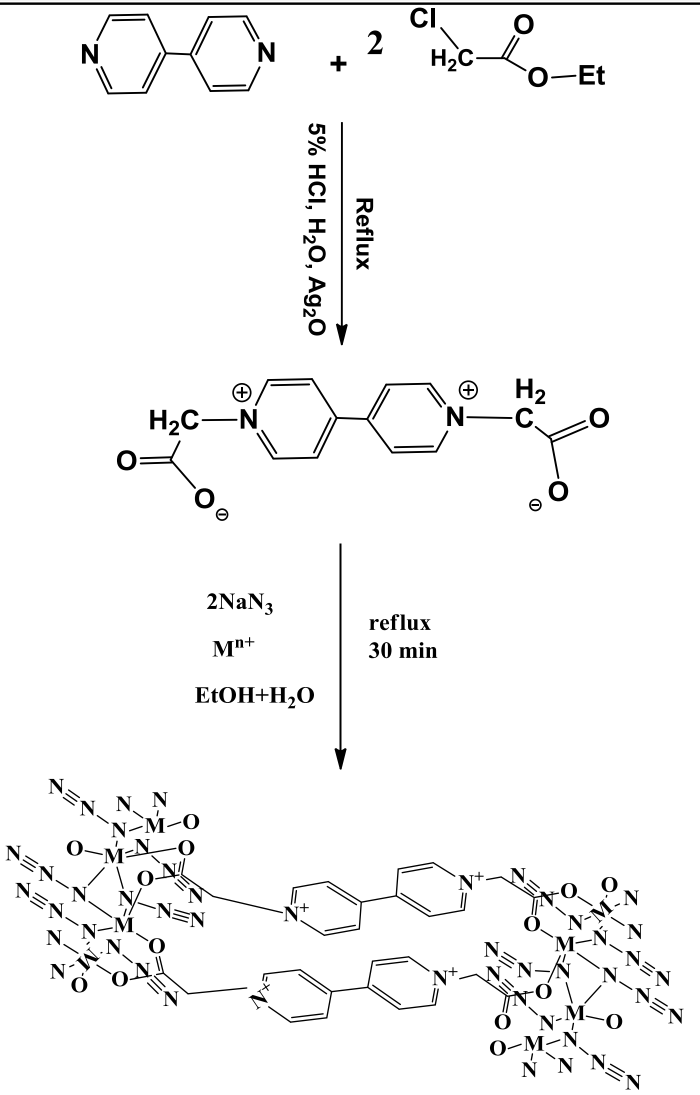

Where: M = Cr^{III}, n = 3; M = Mn^{II}, Fe^{II}, Co^{II}, Ni^{II}, Cu^{II}, Zn^{II}, Cd^{II}, n = 2; M = Ag^{I}, n = 1.

Scheme 1: Synthesis route of ligand and the proposed polymeric complexes.

IR Spectra:

The important infrared bands for the ligand and their complexes together with their assignments are listed in Table 2. The IR spectrum of the ligand shows characteristic bands at 1634 and 1468 assigned for ν_{as}(COO) and ν_{s}(COO), respectively [17-18]. Bands at 1611 and 1593 cm^{-1} are due to the ν(C=N) [19] and ν(C=C) [20], respectively. Bands at 3038 and 2913 cm^{-1} were assigned to the ν(C–H) stretching of the aromatic and aliphatic, respectively [21]. The IR spectra of the complexes exhibited ligand bands with the appropriate shifts and the M-O and M-N frequencies due to complex formation (Table 2). The IR spectra of the polymeric complexes display the ν_{as}(COO) stretching bands around 1603 - 1629 cm^{-1} and ν_s(COO) stretching bands around 1404 - 1458 cm^{-1}. These bands are shifted to lower frequency compared with that in the free ligand. This can be attributed to delocalisation of metal electron density (t_{2g}) to the π-system of the ligand. The difference between ν_{as}(COO) and ν_s(COO) is characteristic for a bidentate coordination mode in which the carboxylato moiety adopts the *syn*-*syn* orientation [22, 23]. Bands at 1560-1643 cm^{-1} are assigned to the ν(C=N) stretch, this band is shifted to lower frequency or to higher frequency compared to that in the free ligand. The shift to lower frequency is due to delocalisation of metal electron density (t_{2g}) to the π-system of the ligand. However, the shift to higher freguency may be indicated a weak interaction between the ligand and metal ion. The appearance of new band at 3395-3462 cm^{-1} may by attributed to hydrated water in the complexes [19] .The strong new bands located at 2037-2112 and 1298-1368 cm^{-1} were attributed to $\nu_{as}(N_3)$ and $\nu_s(N_3)$, respectively [25] . The bands at 1179-1229 cm^{-1} can be attributed to ν(C-N) stretching [26]. At lower frequency the complexes exhibited bands around 401-499 and 503-600 cm^{-1} assigned to ν(M-N) and ν(M-O), respectively [27] . The appearance of ν(M–O) at frequency higher than that of ν(M–N) due to the larger dipole moment change for M–O compared to M–N, the ν(M–O) usually appears at higher frequency than the ν(M–N) band [28] .

Mass Spectra:

The mass spectrum of the ligand was consistent with the proposed structural formulae (see Experimental section). The positive ion MALDI mass spectra for several complexes were reported. The mass spectrum of $[Cd_2(L)(N_3)_4].H_2O$, Figure 5, showed several peaks corresponding to successive fragmentation of the molecule. Scheme 2 represents the fragmentation pattern of the complex. The complex showed no peak related to parent ion. Peak observed at m/z 641.42 (63 %) $(M\text{-}N_3)^+$ represents the molecular ion peak of the complex upon losing N_3 moiety. Other distinct peaks were observed in the mass spectrum at m/z 613.14, 579.13 and 537.11 can be assigned to the $(M\text{-}(N_3+CO))^+$, $(M\text{-}(N_3+CO+H_2O_2)^+$ and $(M\text{-}(N_3+CO+H_2O_2+N_3)^+$ fragments, respectively. The spectrum of $[Ni_2(L)(N_3)_4].H_2O$, Figure 6 and Scheme 3, displayed peak at m/z = 574.11 (9 %), represents the molecular ion peak of the complex. Other distinct peaks were observed in the mass spectrum at m/z 485.94 (9 %) (M-

$(N_2+CO+N_2H_4)^+$, 410.22 (16 %)$(M\text{-}(N_2+CO+N_2H_4+Ni+NH_3))^+$, 324.18 (8 %) $(M\text{-}(N_2+CO+N_2H_4+Ni+NH_3+2CO+N_2H_2))^+$, 270.15 (3 %) $(M\text{-}(N_2+CO+N_2H_4+Ni+NH_3+2CO+N_2H_2+N2+CN))^+$. These results are similar to those of analogous complexes reported earlier by others [29].

Electronic spectra and magnetic moment measurements:

The UV-Vis spectrum of L exhibits a high intense absorption peak at 268 nm, assigned to the overlapping of $\pi \rightarrow \pi^*$ and $n \rightarrow \pi^*$ transitions [30]. The electronic spectrum of the Cr(III) complex shows a high intense peaks at 271 nm due to intra-ligand. The low intense peaks at 604 and 405 and nm were attributed to the $^4A_2g^{(F)}\rightarrow{}^4T_2g^{(F)}$ (ν_1) and $^4A_2g^{(F)}\rightarrow{}^4T_2g^{(F)}$ (ν_2) transition, respectively. These bands attributed to the spin allowed d-d transition [31], indicating octahedral geometry around the Cr(III) atom [32] .The electronic spectra of the Mn (II) complex shows three peaks at 377 nm due to intra-ligand, 379 nm due to charge transfer and at 576 nm assigned to $^6A_1g\rightarrow{}^4T_2g^{(G)}$ transition [33, 34]. Electronic transition peaks of the other complexes confirmed octahedral geometries around metal atoms. Electronic data are summarised in Table (3). The d^{10} complexes exhibited bands at 272; 386, 264; 362 and 267; 307 nm, respectively which assigned to the ligand field and charge transfer transitions for Zn(II), Cd(II) and Ag(I) complexes, respectively. The room temperature magnetic moments of the complexes are reported in Table (3). They show magnetic moments in the range 0.83–2.61 BM. The very low observed moments are allowed us to conclude safely that the complexes are antiferromagnetic [35-37].

3D molecular modelling and analysis of bonding modes:

Molecular simulation attempts to reproduce molecular geometries, energies and other features by adjusting bond lengths, bond angles and torsion angles to equilibrium values that are dependent on the hybridisation of an atom and its bonding fashion. In order to obtain estimates of structural details of these complexes and in view of the six-coordination of all the complexes, we have optimised the molecular structure of the ligand and its polymeric metal-complexes and we have included $[Cr^{III}_2(L)(N_3)_4]Cl_2.H_2O$ as a representative compound (Figure 9). The detail of bond lengths and bond angles per the 3D molecular structure is given in Table 4. Energy minimisation was repeated several times to find the global minimum [38]. The energy minimisation value for octahedral and without restricting the structure for the prepared M-compounds are presented in (Table 4). The molecular modelling for the modulated Cr(III)-complex (Figure 7 and Table 4) shows the bond lengths bond angles around Cr atom, indicating a distorted octahedral geometry around Cr(III) ion [39], and thus the proposed structure of the Cr(III)-complex is acceptable.

Conclusion:

In this paper, we have explored the synthesis and coordination chemistry of some carboxylato-azido metal-complexes derived from the reaction of the multidentate ligand L with a range of metal ions. The ligand behaves as a neutral species upon complexation with the involvement of the nitrogen atoms of the azido groups in coordination for all complexes. The prediction of the formation of six-coordinate polymeric species was based on; the low solubility of the complexes in organic solvents; the low magnetic susceptibility of the complexes; and the electronic spectra of the complexes.

References

1. T. Tanase, J. W. Yun, S. J. Lippard, ***Inorg. Chem***., 35, 3585, (1996).
2. M. Melnik, M. Koman, D. Hudecov, J. Moncol, B. Dudov, T. Glowiak, J. Mrozinski, C. E. Holloway, ***Inorg. Chem. Acta***, 308, (2000)
3. D. Aiello, R. Aiello, F. Testa, T. Martino, I. Aiello, M. L. Deda, M. Ghedini, ***J. Photochem. Photobio***. A. 201, 81-86, (2009).
4. V. K. Garripelli, J. K. Kim, S. Son, W. J. Kim, M. A. Repka, S. Jo, ***Acta Biomater***., 7, 1984-1992, (2011).
5. A. L. Pochodylo, R. L. LaDuca, ***Inorg. Chem. Comm***., 14, 722-726, (2011).
6. S. R. Batten, R. Robson, ***Angew. Chem., Int. Ed***., 37, 1460, (1998).
7. L. Carlucci, G. Ciani, D. M. Proserpio, ***Coord. Chem. Rev***., 246-247, (2003).
8. S. R. Batten, ***Cryst Eng Comm***., 3, 67, (2001).
9. X-J Kong, X-J Long., L-S Long ., Z-P Zheng., R-B Huang, L-S Zheng, ***Acc. Chem .Res***., 43, 201-209, (2009).
10. E-Q Gao, Y- F Yue , S-Q Bai , Z-Yan He.. ***J. Am. Chem. Soc***., 126, 1419, (2004).
11. P. P Liu, A. L. Cheng, N. Liu, W. W. Sun, E. Q. Gao, ***Chem. Mater***., 19, 2724, (2007).
12. X. Y. Wang, L. Wang, Z. M. Wang, S. Gao, ***J. Am. Chem. Soc***., 128, 674, (2006).
13. Y. Z. Zhang, H. Y. Wei, F. Pan, Z. M. Wang, Z. D. Chen, S. Gao, ***Angew. Chem. Int. Ed***., 44, 5841, (2005).
14. Jiang-Gao Mao, Hong-Jie Zhang, Jia-Zuan Ni, Shu-Bin Wang, Thomas C. W. Mak, ***Polyhedron***, 18, 1519-1525, (1999).
15. CS Chem 3D Ultra Molecular Modelling and Analysis, Cambridge, www. cambridgesoft.com.

16. R. C. Maurya, S. Rajput, ***J. Molecular Structure***, 794 24-34, (2006) (molecular modelling).
17. Geary W.J., Coord. Chem. Rev., 7(1971) 81.
18. V. Zelenak, Z. Vargova, K. Gyoryova, ***Spectrochemica Acta***, 66, 262-272, (2007).
19. Li-Fang Song, Chun-Hong Jiang, Cheng-Li Jiao, Jian Zhang, Li-Xian Sun, Fen Xu, Wan-Sheng You, Zhong-Gang Wang and Ji-Jun Zhao, ***Crystal Growth & Design***.Vol. 10, No. 12, (2010).
20. Guang-Xiang Liu, Kun Zhu, Huan-Min Xu, Sadafumi Nishihara, Rong-Yi Huang and Xiao-Ming Ren, ***Cryst Eng Comm***, 12, 1175-1185, (2010).
21. Qi Ma, Miaoli Zhu, Liping LuSisi Feng and Juanzhi Yan, ***Inorg. Chem. Acta***, 370, 102-107, (2011).
22. Al-Jeboori, M.J., Al-Dujaili, A.H. and Al-Janabi, A.E., ***Transition Met. Chem***., 34, 109 (2009).
23. Livingston, S.E., Mayfield, J.H., Moorse, D.S., ***Aust. J. Chem***., 28 (1975) 2531.
24. El-Sonbati, A.Z., El-bindary A.A., Al-Sarawy, A.A., ***Spectrochim Acta Part A***, 58, 2771, (2002).
25. Sandip Mukherjee, Bappaditya Gole, Yo Song and Partha Sarathi Mukherjee, ***Inorg .Chem***., 50, 3621-3631, (2011).
26. Robert M. Silverstein, ***Spectrometric identification of organic compounds*** 7th edition, John Willey and Son, inc., p 174, (2005).
27. N. Raman, S. Esther, C. Thangaraj , ***J. Chem. Soc***., 116(4), 209, (2004).
28. Nakamoto, K., and Ohkaku, N., ***Inorg. Chem***., 10, 798, (1971).
29. F. Mevellec, S. Collet, D. Deniaud, A. Reliquet, J. –C. Meslin, J. Chem. Sic., Perkin Trans.1, 3128, (2001).
30. W. Kemp, "*Organic Spectroscopy*". 2nd, Edition., (1987).
31. Mohamad Jaber Al-Jeboori, Ahlam Jamil Abdul-Ghani and Ahmed Jassim Al-Karawi, ***Transition Met Chem***, 33, 925-930, (2008).
32. S. Chandra, M. Pundir, ***Spectrochim Acta***, Part A, 69, 10.1016, (2007).
33. Mohamad Jaber Al-Jeboori, Amar H. Al-Dujaili and Alyaa E. Al-Janabi, ***Transition Met. Chem***, 34, 109-113, (2009).
34. A. Z. El-Sonbati, A. S. Al-Shihri and A. A. El-Bindary, ***Spectrochemica Acta*** Part A., 60, 1763, (2004).
35. H. C. Zhang, L. N. Zakharov, S. K. Das, M. M. Hetu, A. L. Rheingold, ***Inorg Chim. Acta***, 360, 1691–1701, (2007).
36. O. Kahn, ***Adv. Inorg. Chem***., 43, 179–259, **(**1995).
37. V. Tangoluis, G. Psomas, C. Dendrinou-Samara, C. P. Raptopoulou, A. Terzis, D. P. Kessissoglou, ***Inorg. Chem***., 35, (1996).
38. Mishra, A. P., Mishra, R.K., Shrivastava, S.P., ***Journal of the Serbian Chemical Soci***ety, 74, 523-535, (2009).

39. Colak, A. T., Irez, G., Mutlu, H., Hökelek, T., Caylak, N., ***Journal of Coordination Chemistry***, 62 (6), 1005-1014, (2009).

Table1: Colours, yields, elemental analyses, and molar conductance values.

Formula	Colour	M.P °C	M.W	Yield (%)%	Micro analysis found (calc)%				
					C	H	N	Metal	Cl
$C_{14}H_{14}Cl_2Cr_2N_{14}O_5$	Green	Dec 340	633.25	67	26.89 (26.55)	2.21 (2.23)	31.02 (30.97)	17.93 (16.42)	12.23 (11.20)
$C_{14}H_{14}Mn_2N_{14}O_5$	Pale yellow	Dec 350	568.23	70	29.16 (29.59)	2.31 (2.48)	35.64 (34.51)	19.17 (19.34)	0.71
$C_{14}H_{14}Fe_2N_{14}O_5$	Brown	Dec 350	570.04	73	28.99 (29.50)	2.35 (2.48)	35.52 (34.40)	19.86 (19.59)	0.77
$C_{14}H_{14}Co_2N_{14}O_5$	blue	Dec 330	576.22	73				19.83 (20.46)	1.01
$C_{14}H_{14}Ni_2N_{14}O_5$	Green	Dec 340	575.74	76	28.13 (29.21)	2.29 (2.45)	35.16 (34.06)	20.31 (20.39)	1.2
$C_{14}H_{14}Cu_2N_{14}O_5$	Green	Dec 313	585.44	78	27.83 (28.72)	2.37 (2.41)	34.56 (33.49)	21.99 (21.71)	1.51
$C_{14}H_{14}Zn_2N_{14}O_5$	yellow	Dec 317	589.13	83				21.52 (22.20)	0.41
$C_{14}H_{14}Cd_2N_{14}O_5$	white	Dec 302	683.17	61				31.42 (32.91)	0.82
$C_{14}H_{14}Na_2Ag_2N_{14}O_5$	white	182	720.07	55				30.93 (29.96)	0.54

(Cala=Calculated) , Dec=Decomposed

Table 2: IR frequencies (cm^{-1}) of the compounds.

Complex	**νO-H**	**νCH$_2$**	**ν$_{as}$N$_3$**	**ν$_{as}$COO**	**νC=N**	**νC=C**	**ν$_s$COO**	**δO-H**	**ν$_s$N$_3$**	**νC-N**	**νM-O**	**νM-N**	**Δ(ν$_{as-}$ν)**
L	-	2913	-	1634	1611	1593	1468	-	-	1231	-	-	166
$Cr_2(L)(N_3)_4]Cl_2.H_2O$	3462	2868	2037	1620	1603	1584 1436	1406	1558	1368	1225	550 588	436 499	206
$[Mn_2(L)(N_3)_4]H_2O$	3422	2872	2038	1603	1560	1560	1404	1518	1338	1179	548 579	442 467	199
$[Fe_2(L^1)(N_3)_4]H_2O$	3414	2859	2102	1629	1553	1528 1456	1412	1501	1298	1229	525	428 455	217
$[Co_2(L)(N_3)_4]H_2O$	3422	2830	2045	1623	1593	1580	1458		1362	1223	541 600	413 27 476	165
$[Ni_2(L)(N_3)_4]H_2O$	3395		2078	1603	1613	1533	1416	1491	1317	1221	563 498	467 498	187
$[Cu_2(L)(N_3)_4]H_2O$	3449	2849	2112	1612	1643	1546	1418	1528	Overlap	1223	505 586	419 453	194
$[Zn_2(L)(N_3)_4].H_2O$	3408	2849	2056	1618	1580	1549 1468	1425	1531	1367	1227	569	444	193
$[Cd_2(L)(N_3)_4]H_2O$	3424	2864	2099	1612	1628	1540	1406	1506	1354	1223	505 532 565	401 453	206
$Na_2[Ag_2(L)(N_3)_4]H_2O$	3406	2941	2083	1612	1641	1641 1466	1418	1551	1302	1225	503 567	419 453	194

Table 3: Magnetic moment, u.v-vis spectral data in DMSO solutions and total minimisation energy.

Compound	μ_{eff} BM per atom	Band Position λ_{nm}	Wave number (cm^{-1})	Extinction coefficient ε_{max} ($dm^3\ mol^{-1}\ cm^{-1}$)	Assignment	Total energy kcal/mol
L	-	268	37313	1130	n →□* and □→□*	-
$[Cr_2(L)(N_3)_4]Cl_2.H_2O$	2.61	271 405 604	36900 24691 16556	639 32 15	Intra-ligand $^4A_2g^{(F)} \rightarrow {}^4T_2g^{(F)}$ (ν_1) $^4A_2g^{(F)} \rightarrow {}^4T_2g^{(F)}$ (ν_2)	124.0233
$[Mn_2(L)(N_3)_4]H_2O$	2.20	277 379 576	36101 26385 1736	850 259 62	Intra-ligand C.T $^6A_1g^{(S)} \rightarrow {}^4T_1g^{(G)}$	122.5619
$[Fe_2(L)(N_3)_4]H_2O$	2.56	273 379 500 681	36630 26385 20000 14684	1460 467 545 11	Intra-ligand C.T $T_2g \rightarrow A_1g$ $^5T_2g \rightarrow {}^5Eg$	102.9585
$[Co_2(L)(N_3)_4]H_2O$	1.93	263 373 652	38023 26810 15337	1931 222 39	L.F C.T $^4T1g^{(F)} \rightarrow {}^4A_2g^{(F)}$	200.4545
$[Ni_2(L)(N_3)_4]H_2O$	1.51	278 639 737	35971 15640 13569	2257 4 8	Intra-ligand $^3T_2g \rightarrow {}^3T_1g^{(F)}$ $^3B1g \rightarrow {}^3B2g$ and $^3B1g \rightarrow {}^3A_2g^a$	668.5644
$[Cu_2(L)(N_3)_4]H_2O$	0.71	268 610 674	37313 16393 14837	450 66 20	Intra-ligand $^2B1g \rightarrow {}^2B_2g$ $^2B_1g \rightarrow {}^2A_2g$	126.5830
$[Zn_2(L)(N_3)_4]H_2O$	-	272 386	36764 25907	1579 57	Intra-ligand C.T	131.4667
$[Cd_2(L)(N_3)_4]H_2O$	-	264 362	37879 27624	1547 11	L.F C.T	112.3343
$Na_2[Ag_2(L)(N_3)_4]\ H_2O$	-	267 307	37453 32573	981 12	L.F C.T	100.0175

Type of Bond	Bond length (A˚)	Type of Bond	Bond angle (˚)
Cr_1-O_1	1.861	C_1-O_1-Cr_1	120.531
Cr_1-N_2	1.856	O_1-Cr_1-N_2	167.369
Cr_1-N_4	1.910	O_1-Cr_1-N_4	93.620
Cr_1-N_3	1.912	O_1-Cr_1-N_3	96.618
Cr_1-N_1	1.876	O_1-Cr_1-N_1	87.811
Cr_1-O_2	1.841	O_1-Cr_1-O_2	84.917
C_1-O_1	1.418	N_2-Cr_1-N_4	89.848
N_4-N_6	1.364	N_2-Cr_1-N_3	95.749
N_3-N_5	1.363	N_2-Cr_1-N_1	90.060
		N_2-Cr_1-O_2	82.695
		N_4-Cr1-N3	85.687
		N_4-Cr_1-N_1	173.706
		N_4-Cr_1-O_2	94.744
		N_3-Cr_1-N_1	88.058
		N_3-Cr_1-O_2	178.387
		N_1-Cr_1-O_2	91.488
		Cr_1-N4-N6	117.436
		Cr_1-N_3-N_5	117.052
		Cr_1-N_4-Cr_2	102.501

		Cr_1-N_3-Cr_2	102.292

Table (4) The calculated bond length and bond angle of $[Cr_2(L)(N_3)_4]Cl_2.H_2O$

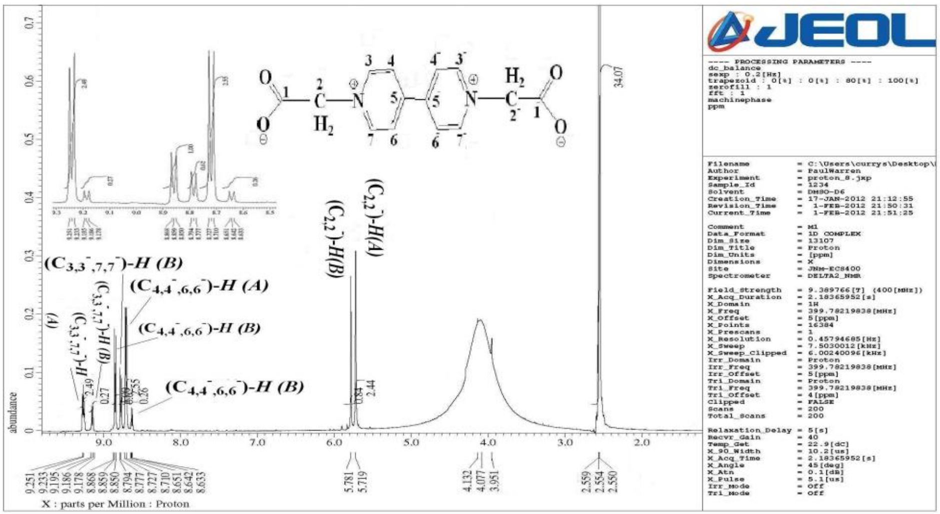

Figure 1: ^{1}H NMR spectrum analysis of L in DMSO-d_6.

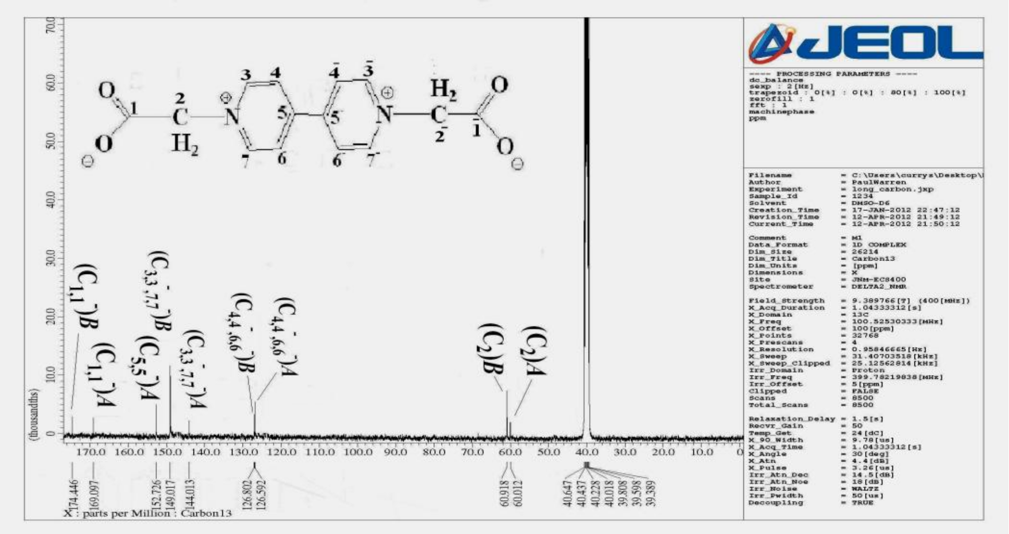

Figure 2: ^{13}C NMR spectrum analysis of L in DMSO-d_6.

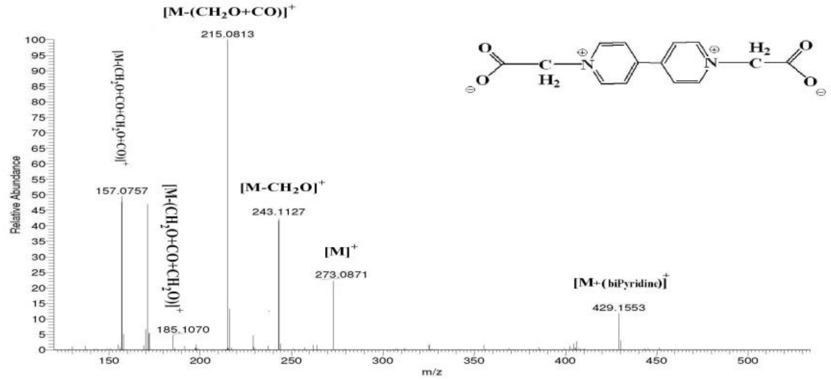

Figure 3: ES (+) Mass spectrum analysis of L.

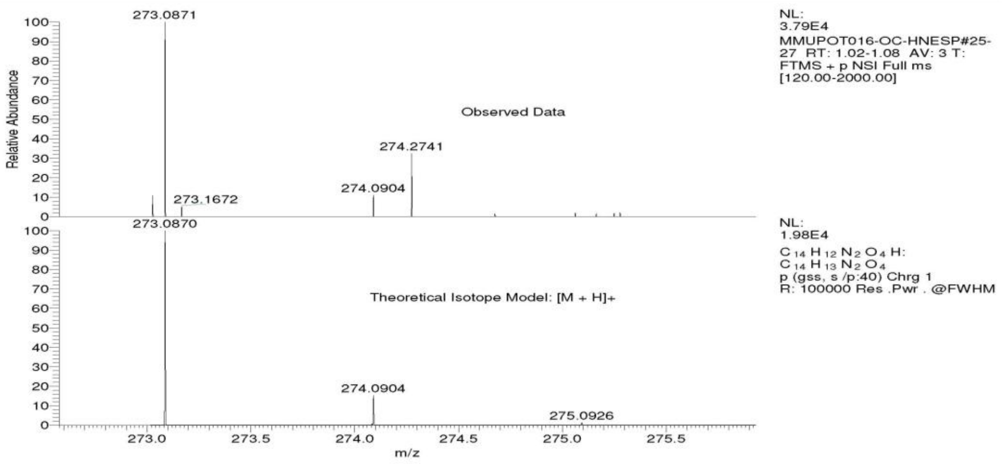

Figure 4: ES (+) Accurate mass spectrum analysis of L.

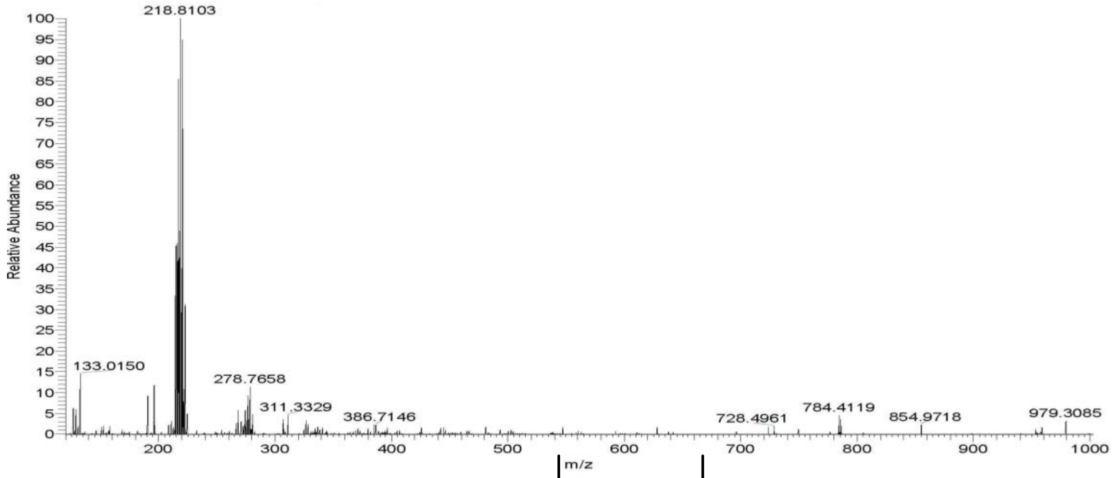

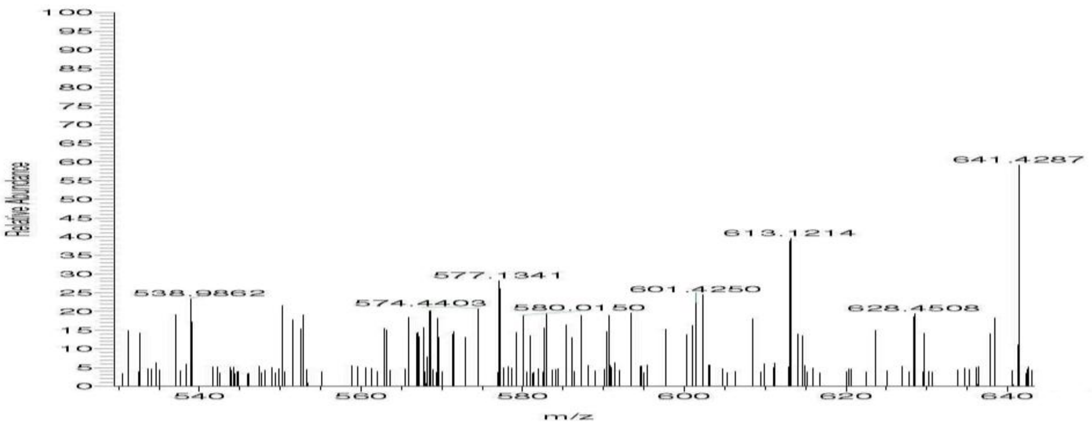

Figure (5) ES (+) Mass spectrum of [$Cd_2(L)(N_3)_4$].H_2O

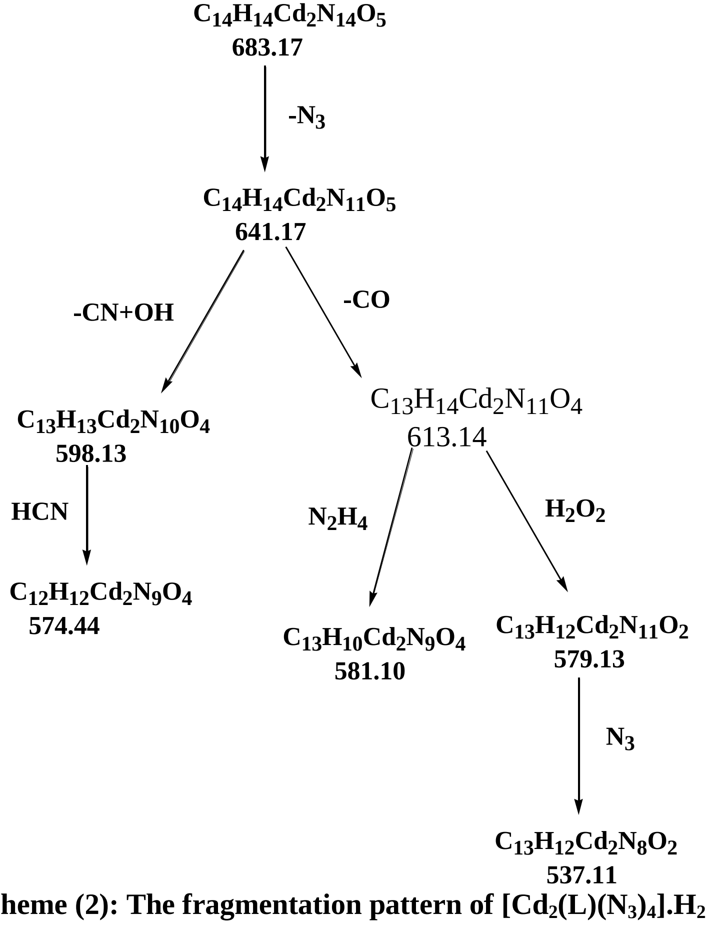

Scheme (2): The fragmentation pattern of [$Cd_2(L)(N_3)_4$].H_2O

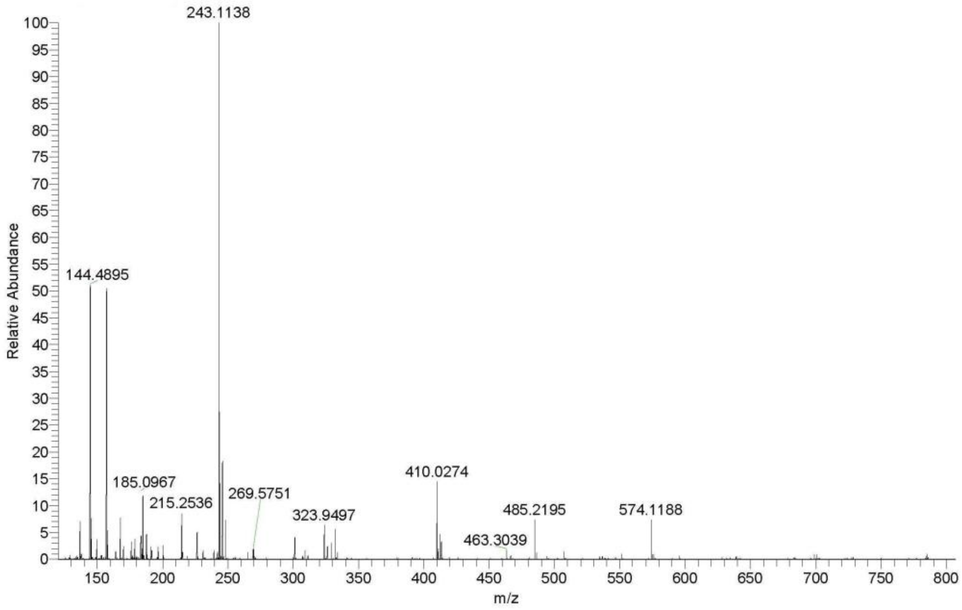

Figure (6): ES (+) Mass spectrum of $[Ni_2(L)(N_3)_4].H_2O$

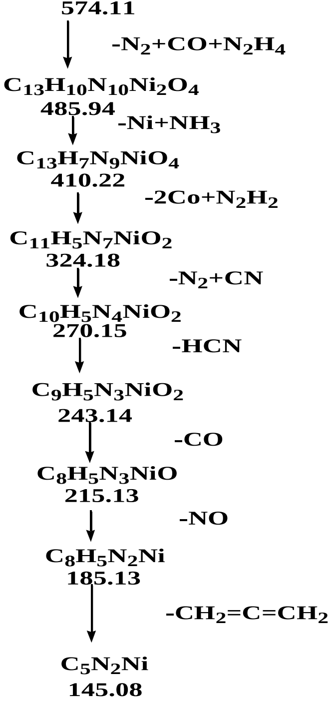

Scheme (3): The fragmentation pattern of $[Ni_2(L)(N_3)_4].H_2O$

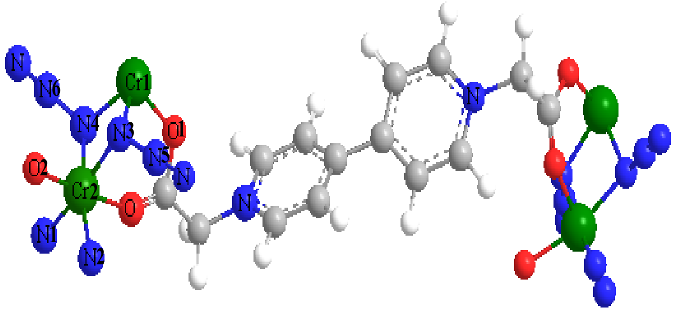

Figure (7): 3D Molecular modelling of complex $[Cr_2(L)(N_3)_4]Cl_2.H_2O$

تكوين تجمعات ذاتية لمعقدات بوليمرية مع جسور ليكاندات الازايد والكاربوكسيلات الثنائية

رياض محمود احمد، احمد ثابت نعمان، تقي الدين عبد الهادي حمدان، محمد جابر الجبوري
قسم الكيمياء ، كلية التربية ابن الهيثم ،جامعة بغداد

الخلاصــــــة

تضمن هذا البحث تحضير معقدات فلزية بوليمرية جسرية سداسية التناسق من تفاعل ٤و٤–ثنائي بيريدين مع اثيل كلورو اسيتيت وبنسبة امولية ٢:١ لتعطي ليكاند كابوكسيلي متعددة الاسنانbis(N-carboxylatomethyl)-4,4`-dipyridinium . ان تفاعل الليكاند مع بعض املاح كلوايدات الفلز الانتقالية وازايد الصوديوم بنسبة ٢:١:١ لتعطي المعقدات البوليمرية المطلوبة. عند تكوين المعقدات، كاربوكسيليت الليكانـد تسلك كاصناف متعددة الاسنان متعادلة. طبيعة الارتباط والشكل الهندسي لهذه المعقدات قد شخصت بواسطة الطرق الكيميائية–الفيزيائية والطــرق الطيفية. اظهرت هذه الدراسات الشكل الثماني السطوح حول المراكز الفلزية والصيغة العامة للمعقــدات المضــرة $[Cr_2(L)(N_3)_4Cl_2].H_2O$ ، , $Na_2[Ag_2(L)(N_3)_4].H_2O$ $[M_2(L)(N_3)_4].nH_2O$ حيث [M(II)= Fe, Co, Ni, Cu, Zn and Cd]. شخصت هذه المركبات بواسطة الاشعة تحت الحمراء الاشعة ، فوق البنفسجية–المرئية ، الرنين النووي المغناطيسي ^1H, ^{13}C NMR ، طيف الكتلــة ، التحليــل الــدقيق للعناصــر C.H.N، الامتصاص الذري ، محتوى الكلور ، الحساسية المغناطيسية ، درجة الانصهار والتوصيلية المولارية. التراكيب الجزيئية لهذه المعقدات حددت بواسطةCS Chem 3D Ultra Molecular Modelling and Analysis Program والتي دعمت الشكل الثماني السطوح.